International Journal of Chemical, Materials and Biomolecular Sciences
ISSN: 2415-6620
Vol:13, No:8, 2019

Triple Intercell Bar for Electrometallurgical Processes: A Design to Increase PV Energy Utilization

Eduardo P. Wiechmann, Jorge A. Henríquez, Pablo E. Aqueveque, Luis G. Muñoz

***Abstract*—**PV energy prices are declining rapidly. To take advantage of the benefits of those prices and lower the carbon footprint, operational practices must be modified. Undoubtedly, it challenges the electrowinning practice to operate at constant current throughout the day. This work presents a technology that contributes in providing modulation capacity to the electrode current distribution system. This is to raise the day time dc current and lower it at night. The system is a triple intercell bar that operates in current-source mode. The design is a capping board free dogbone type of bar that ensures an operation free of short circuits, hot swapability repairs and improved current balance. This current-source system eliminates the resetting currents circulating in equipotential bars. Twin auxiliary connectors are added to the main connectors providing secure current paths to bypass faulty or impaired contacts. All system conductive elements are positioned over a baseboard offering a large heat sink area to the ventilation of a facility. The system works with lower temperature than a conventional busbar. Of these attributes, the cathode current balance property stands out and is paramount for day/night modulation and the use of photovoltaic energy. A design based on a 3D finite element method model predicting electric and thermal performance under various industrial scenarios is presented. Preliminary results obtained in an electrowinning facility with industrial prototypes are included.

***Keywords*—**Electrowinning, intercell bars, PV energy, current modulation.

I. Introduction

THE current technological breakthrough in PV systems has caused a drop in electricity prices. Since 2010, the price of PV generation has drop from USD 210 to USD 18 [1]. This rapid decrease in energy prices will come in hand with a revolution in the way the industry takes advantage of PV energy cost. Depending on the area in which the PV plant is set, PV plants supply energy to the grid between 9 am and 5 pm (see Fig. 1).

The proper operation of copper electrowinning (EW) cells requires good current balance to ensure low dispersion in copper deposition on the cathode plates over time. This requires an intercell bar with intrinsic resilience to contacts wear, electrode misalignment and electrolytic impurities [2], [3]. This paper presents an improved current distribution system that fulfills this purpose by forcing current balance among cell cathodes [4]. The equalization of equivalent resistances is accomplished thanks to a series electrical connection. The system comprises a polymer composite baseboard, S-shaped copper main busbars and U-shaped secondary bars.

This work was supported by the Chilean research fund CONICYT under FONDAP project Nº 15110019.

Eduardo P. Wiechmann F. is with the Electrical Department of University of Concepcion, Chile (corresponding author, phone: 56-41-2204775; e-mail: eduardo.wiechmann@udec.cl).

Jorge A. Henriquez M., Pablo E. Aqueveque N. and Luis G. Muñoz Q.are with the University of Concepción, Chile (e-mail: jorhenriquez@udec.cl, pablo.aqueveque@udec.cl, luismunoz@udec.cl).

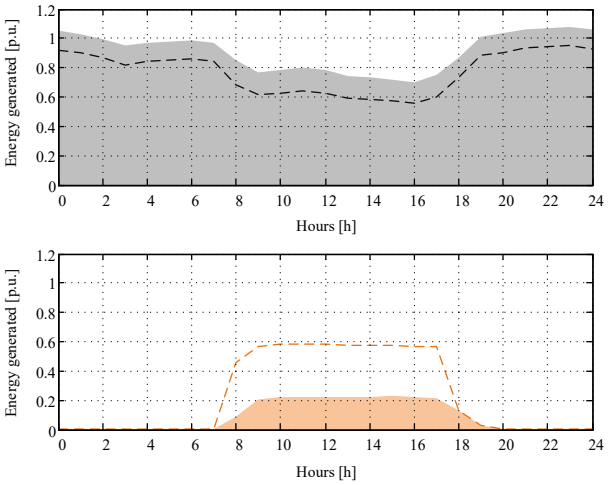

Fig. 1 Daily generation pattern 09-16-2017 of the Great North Interconnected System (SING). Fossil fuels based (grey) and PV energy (orange). Dotted line represents the projected change if EW facilities if modulated to utilize PV energy (±25%)

This work presents a design of a dog-bone type system, designated as Triple Intercell Bar (TIB). The design criteria ensure a colder operation to reduce copper corrosion and annealing. The operational temperature of the system improves based on the removal of the capping board. Zaldívar Mining Company (Antofagasta, Chile) is currently evaluating industrial prototypes.

II. The Busbar Topology

The busbar topology should meet strict requirements to modulate the process and incorporate PV energy, according to the following hierarchy:

1. Operate with high current balance.
2. Ensure current flow facing anomalies.
3. Control metallurgical short circuits.
4. Ensure copper deposit facing contact loss.

5. Design to prevent the entrapment of anti-mist spheres between the electrodes and busbars
6. Provide adequate heat dissipation.
7. Lower the corrosion and contact warp
8. Simplify bar repair.
9. Provide proper electrode spacing.

Fig. 2 shows the experimental prototype (suitable for asymmetrical anodes) and the industrial prototype under evaluation (suitable for symmetrical electrodes).

The main S-shaped segments connect one-to-one anodes and cathodes for current equalization and limiting short circuits [5] (see Table I). U-shaped secondary bars connect the otherwise insulated ends of the electrodes. To attach U-shaped bars to the polymeric base, the TIB uses nuts embedded and anchored inside the base and PTFE bolts. U-shaped secondary connectors provide an alternate path for currents to ensure current flow and copper deposition. Being equipped with these secondary connectors, the TIB can cope with industrial challenges including: open circuit due to loss of contact between an electrode and the main busbar (blanks generation), and over-temperature in faulty ("dirty") contacts and metallurgical short-circuit control (see Table I) [6].

TABLE I
CONVENTIONAL AND TIB COMPARISON @ 45ºC PROCESS TEMPERATURE

Parameter	Conventional	TIB
Current dispersion	15,4%	8,9%
Nominal operation voltage	~2.00 V	~1.9 V
Nominal depositing current density	330 A/m^2	330 A/m^2
Increment over electrolyte temperature	35 °C	0 °C
Short circuit operation voltage	~1.98 V	~1.6 V
Cathode over-current facing short circuit	1,200 A	300 A
Over-temperature facing short circuit	145 °C	35 °C
Depositing current facing open circuit	0 A/m^2	200 A/m^2
Over-temperature facing open circuit	35 °C	10 °C

The capping board free topology provides better heat dissipation and lower operational temperature (from 75 °C to 55 °C). This translates in lower corrosion, lower contact warp, and lower contact cleaning requirements per harvest.

Fig. 2 TIB prototype

III. COMPUTATIONAL MODELS

Two models test the design and predict its electrical and thermal behavior. A concentrated parameter model determines the current dispersion in an EW facility and a finite element model explains the electrical and thermal phenomena.

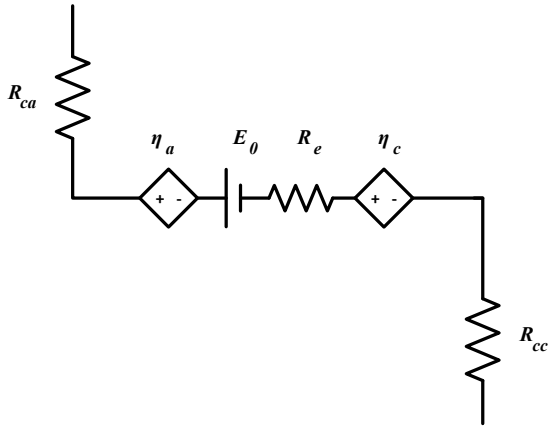

Fig. 3 Parameter concentrated model of an anode-cathode pair in copper EW

A. Current Dispersion Concentrated Parameter Model

Resistances and voltage sources compose an equivalent circuit for the EW process (see Fig. 3).

Contact resistances represent the losses in the contact area (anode and cathode). Electrolyte resistance represents the ohmic losses in the electrolyte. The voltage source E_0 represents the activation voltage (~0.89 for copper EW) and η_c and η_a represent the cathodic and anodic overvoltage's, expressed by Butler-Volmer equation (1) [6].

$$i_{loc,m} = i_0\left(\exp\left(\frac{\alpha_a F \eta_a}{RT}\right) - \exp\left(\frac{\alpha_c F \eta_c}{RT}\right)\right) \quad (1)$$

A matrix of admittances **Y** represents the equivalent circuit of the EW facility. The equation system is solved according to (2):

$$\mathbf{V} = \mathbf{Y}^{-1}\mathbf{I} \quad (2)$$

B. FEM Modeling

Multiphysics analysis is a powerful tool to deal with copper EW. Modeling must consider four physically interactive phenomena: electrochemical, electrical, thermal and fluid dynamics (ventilation) [7]. A finite element model assembles these phenomena to predict the behavior of key process variables.

The Ohm's law describes the current density in the electrolyte as,

$$\mathbf{i}_l = -\sigma_l \nabla \phi_l \quad (3)$$

where the conductivity is,

$$\sigma_l = F^2 \sum z_i^2 u_{m,i} c_i \quad (4)$$

For the electrode, the Ohm's law is,

$$\mathbf{i}_s = -\sigma_s \nabla \phi_s \tag{5}$$

The primary current distribution considers the voltage drop due to the electrolyte resistance. The secondary current distribution considers the voltage drop in the interphase electrode-electrolyte according to the Butler-Volmer equation [8].

The Ohm's law describes current density as,

$$\mathbf{J}_{ec} = \sigma \mathbf{E} = -\sigma \nabla \mathbf{V} \tag{6}$$

In addition, a stationary system must fulfill the Laplace equation

$$\nabla \mathbf{J}_{ec} = \nabla(-\sigma \nabla \mathbf{V}) \tag{7}$$

It is necessary to define a ground, where the voltage is zero volts. For this purpose, the end of the anode hanger-bar is the ground.

Finally, the inner current for the electro-chemistry model is the outer current of the electrical busbar model, according to:

$$\int_{\partial\Omega} \mathbf{J}_{ec} \cdot \mathbf{n} dS = I_{s,total} \tag{8}$$

The heat dissipation for any solid element in the model is,

$$\rho C_p \nabla T = k \nabla^2 T + Q \tag{9}$$

The heat dissipation in the contacts between electrodes and the busbar is,

$$-\mathbf{n} \cdot (-k \nabla T) = Q_s \tag{10}$$

The heat sources come from the electrical busbar model, where the heat external source is,

$$Q = \oint_{\partial\Omega} -\nabla \mathbf{V} \cdot \mathbf{J} \cdot d\Omega \tag{11}$$

The ventilation system is by airflow at room temperature (typically 20 °C) driven by fans passing sideways by the cells. The air model is an air block with a laminar flow. The Navier-Stokes equations for continuity (10) and impulse (11) for single-phase fluids describe the ventilation system,

$$\nabla(\rho \mathbf{u}) = 0 \tag{12}$$

$$\rho(\mathbf{u} \cdot \nabla \mathbf{u}) = \nabla \cdot \left[-p\mathbf{I} + \mu\left(\nabla \mathbf{u} + (\nabla \mathbf{u})^T\right) - \frac{2}{3}\mu(\nabla \cdot \mathbf{u})\mathbf{I} \right] + \mathbf{F} \tag{13}$$

At the inlet, the air velocity is set to 1.0 m/s with a temperature boundary condition set at 20 °C and a heat outlet at the other end,

$$-\mathbf{n}(-k \nabla T) = 0 \tag{14}$$

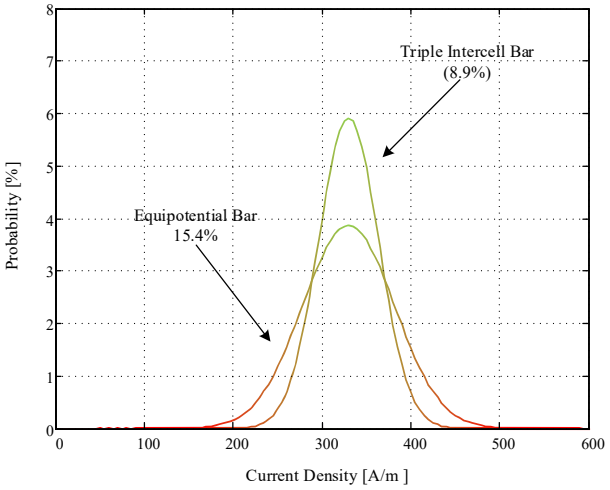

Fig. 4 Comparison of current dispersion of equipotential bar and triple segmented bar

IV. TIB Attributes

A. Current Balance

The current balance is associated with the process current efficiency [5]. The concentrated parameter model predicts the current dispersion of the electrodes on a cell.

Different configurations of intercell connections exhibit different current dispersions. Equipotential busbars operate with a current dispersion of 15.4%, while TIBs operate with 8.9%.

B. Current Flow during Anomalies

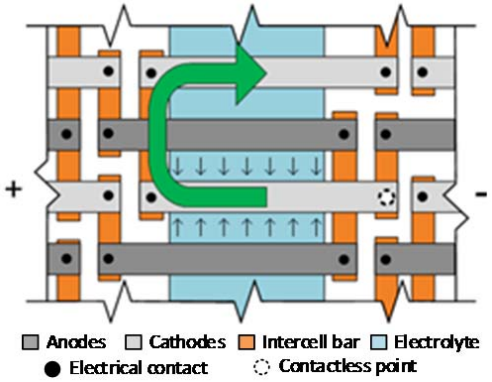

Fig. 5 Overview of current flow in an EW cell facing a loss of electrical contact between cathode and busbar

When the hanger-bar loses electrical contact with the busbar, an open circuit occurs. Therefore, this anomaly inhibits copper deposit in the cathode. The inclusion of the auxiliary U-shape connectors provides an alternative low-resistance path for the current to flow, with the otherwise insulated end of the hanger-bar (see Fig. 5). In this way, current comes into the cell through the anodes, passes across the electrolyte to the cathode. The current flows through the opposite end of the cathode´s hanger-bar using the U-shape connector and through the hanger-bar of the cathode of the

next cell. Therefore, U-shape auxiliary connector provides a backup connection. This reduces power losses and ensures copper deposit and low dispersion of cathode currents.

In the presence of an impaired contact, its resistance increases. Equipotential cannot surpass this anomaly. The TIB innovation provides a secondary path through the U-shaped connectors. This connector acts in the same way as before when facing a loss of electrical contact. In the cathode, a small fraction of the depositing current flows directly to the next cell through the impaired contact and the rest flows through the U-shaped connector. In this case a fraction of the current coming from the electrolyte passes through the U-shaped connector to the hanger bar of the other connected cathode to the next cell.

C. Overcoming Process Anomalies

The segmented nature of the main busbar (S-shaped connectors) provide an inherent metallurgical short-circuit protection [4], [5]. TIB uses a "series" connection between electrodes, thus generating series resistance paths. These paths limit over-currents by limiting the short-circuit with the contribution of the resistances of the adjacent cells. With an equipotential busbar over-currents in a short-circuited electrode can reach 1,200 A, while TIB limits over-currents to 300 A. Facing metallurgical short-circuits, over-temperature reaches +145 °C in equipotential busbars whereas in TIB only +35 °C. This effect becomes evident with the FEM thermal profile (see Fig. 6).

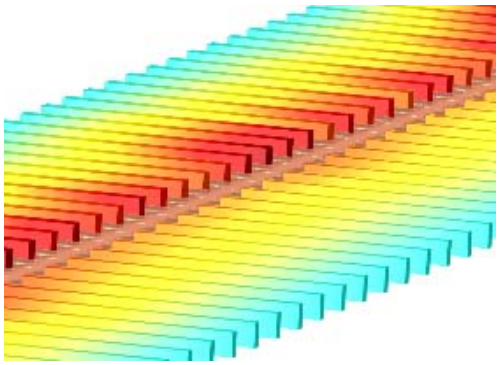

(a)

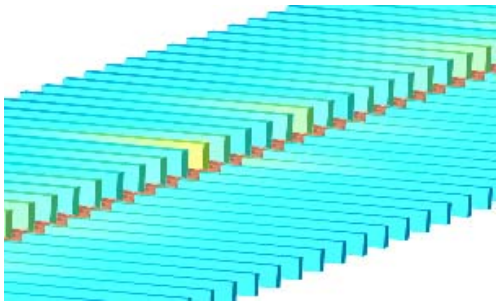

(b)

Fig. 6 Thermal profile facing a metallurgical short-circuit (a) Equipotential busbar, (b) TIB

To ensure the flow of current facing impaired or open contacts TIB uses U-shaped auxiliary connectors. U connectors provide up to 60% of the process current to the cathode facing a loss of electrical contact (open circuit). Also, U connectors provide up to 72% of the process current facing a partial loss of electric contact (impaired or dirty contact). Avoiding blanks prevents excessive deposit in adjacent electrodes and reduces the formation of short circuits.

D. Spheres Entrapment

Frequently EW plants use plastic spheres to reduce acid mist. In the process of harvesting the cathodes, some spheres end up falling over the busbar and get trapped between the busbar contact and the capping board (see Fig. 7). Later on, these spheres prevent the electric contact during permanent cathodes reposition. TIB geometrical design and its baseboard help to avoid this issue (see Fig. 2).

E. Corrosion and Annealing Issues

During the lifetime of an intercell busbar, it is exposed to a highly aggressive environment that shortens its lifespan. Three factors contribute:

1. Overheating induced by metallurgical short-circuits,
2. Open circuits and impaired contacts [9].
3. Mechanical stress.
4. Corrosion caused by the acid mist.

A 3D finite element model predicts efficiencies and thermal profiles for both: the equipotential busbar and TIB.

Fig. 7 Silicone sphere entrapped in an equipotential busbar

The results show a correlation between current dispersion and the efficiency of the process [2], [5]. Also, lower current dispersion results in lesser power losses in the busbar and cooler operational temperature. Busbar's power losses (15) are the sum of the contact power losses and the copper conductive losses (see Figs. 1 and 2).

$$P = \sum_{i=1}^{n} \left(I_{c_i}\right) R_{cc_i} + \sum_{i=1}^{n} \left(I_{a_i}\right) R_{ca_i} + P_{bulk} \tag{15}$$

Minimizing the first term in (15) results in (16):

$$I_{c_i} \cdot R_{cc_i} = I_{c_n} \cdot R_{cc_n} \tag{16}$$

Currents should be equalized to minimize power losses in the electrode contacts and conductive elements.

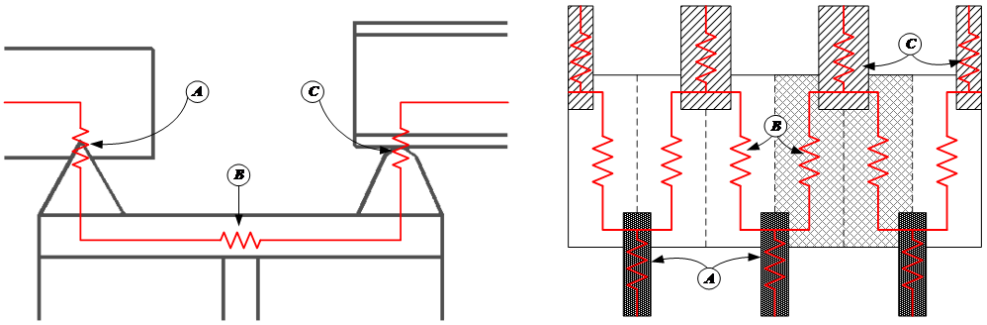

Fig. 8 Electrical equivalent for an intercell busbar: Anode contact resistance (a); copper bulk resistance (b); cathode contact resistance (c)

Alternative configurations of intercell connections provide different current dispersions. Equipotential busbars operate with a 15.4% current dispersion while segmented busbars achieved 8.9%.

Industrial measurements confirm a correlation between current dispersion and the energy efficiency of the process. This also stands for the power dissipated at the bar.

Currently, the typical equipotential dog-bone busbar uses contacts 14 cm apart. However, these busbars do not have a good heatsink area. Without proper ventilation the operational temperature works with +35 °C above electrolyte temperature.

TIB offers a larger heatsink area (120 cm^2). Computational simulations show slight increase of temperature above electrolyte temperature (see Fig. 9). The thermal profile obtained 3D FEM model is consistent with the industrial thermal image.

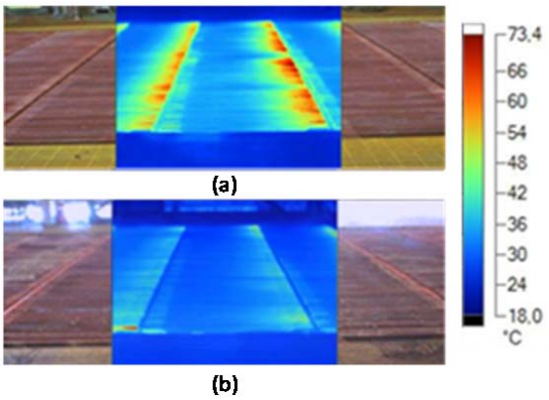

Fig. 9 Thermal image from an EW cell using alternative intercell busbar configurations: (a) Equipotential, (b) TIB

The loading process of the electrodes into the cell produces a mechanical stress on the contacts. If the copper contacts are annealed it will result in local busbar damages (see Fig. 11).

Since TIB overcomes anomalies and corresponding copper annealing, the lifetime of the contacts is improved.

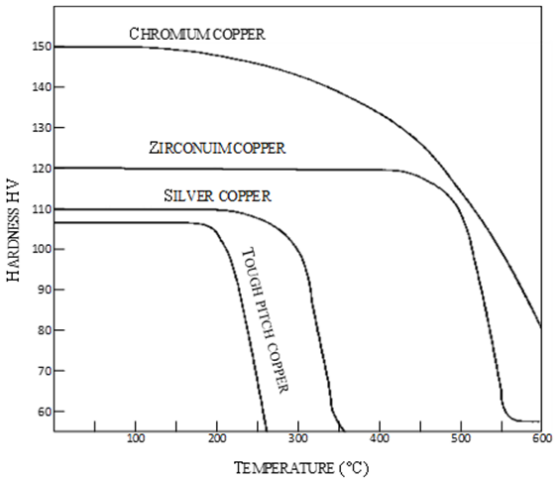

Fig. 10 Hardness of different copper alloys

Fig. 11 Damaged copper contact in an equipotential dogbone busbar

F. Simplified Repair

High operational temperatures, acid mist corrosion and mechanical stresses deteriorate the copper intercell bar [9]-[11]. The TIB capping-board free design allows the replacement of any S-shape segment without interrupting the current of the process. The replacement of a segment takes is a cost-effective solution compared with the replacement of a bar.

G.Electrode-Spacing Baseboard

Metallurgical short-circuits occurrence increases with high electrolyte resistance dispersion. Electrolyte resistance depends highly on electrodes distance [5], [9]. The proposed base-board design of the TIB provides electrodes support and proper spacing. Furthermore, the elimination of the capping-board improves ventilation of the S-shape segments reducing its operational temperature and corrosion rate.

V. Discussion

Increasing 20% the process current with the support of TIB technology can be done without compromising the intercell operational temperature (see Fig. 12) and/or the current balance (see Fig. 13). For a production cycle, the current should be increased and decreased several times (see Fig. 14) following the PV generation pattern.

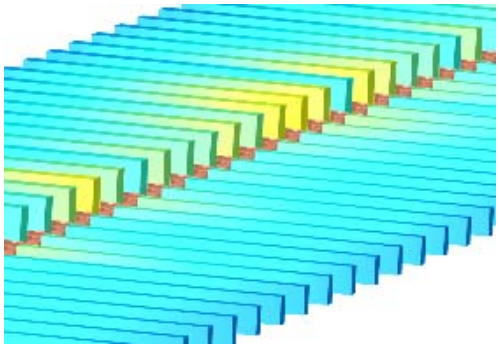

Fig. 12 TIB thermal profile with +20% above rated current

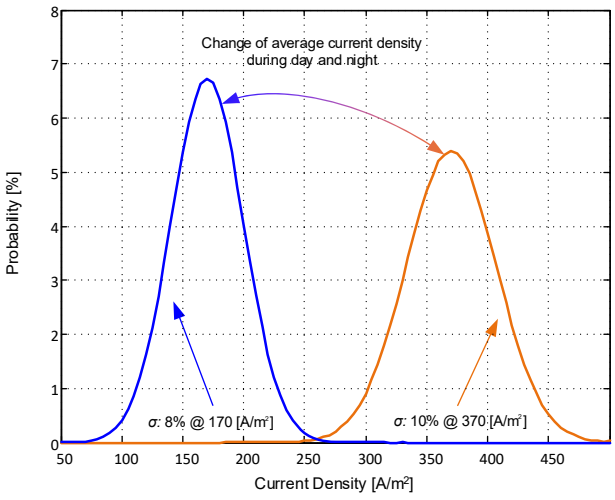

Fig. 13 Current dispersion on daylight and night

VI. Conclusion

TIB provides technology to ensure deeper daylight utilization to take advantage of PV energy. With TIB process anomalies are overcome, and current dispersion is reduced. It is predicted that the process current can be increased by 20% above its rated value. This also means that industrial facilities working with lower currents should modulate up that level to take full advantage of PV.

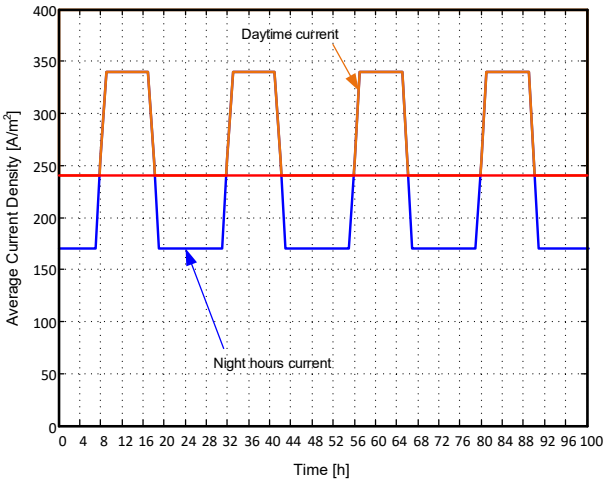

Fig. 14 Current density profile when modulating process current

References

[1] International Renewable Energy Agency, “Renewable Energy Auctions 2016”, 2017.

[2] M. E. Schlesinger, M. J. King, K. C. Sole, W. G. Davenport, "Extractive Metallurgy of Copper (Fifth Edition)", Elsevier Ltd., UK, 2011.

[3] M. Free, M. Moats, G. Houlachi, E. Asselin, A. Allanore, J. Yurko, S. Wang, "Electrometallurgy 2012", John Wiley & Sons, USA, 2012.

[4] E. P. Wiechmann, G. Vidal, A. Pagliero y J. Gonzalez, «Copper Electrowinning using Segmented Intercell Bars for Improved Current Distribution, » Canadian Metallurgical Quarterly, vol. 41, nº 4, pp. 425-432, 2002.

[5] Aqueveque, P.E.; Wiechmann, E.P.; Herrera, J.; Pino, E.J., "Measurable Variables in Copper Electrowinning and Their Relevance to Predicting Process Performance," in Industry Applications, IEEE Transactions on, vol.51, no.3, pp.2607-2614, May-June 2015

[6] Doren, N.A.; Hoffman, M.A., “Clarifying the Butler–Volmer equation and related approximations for calculating activation losses in solid oxide fuel cell models”, Journal of Power Sources, vol. 152, pp. 175-181, May 2005.

[7] I. S. Laitinen, H. K. Virtanen, O. T. Järvinen, T. M. Kumara y J. T. Tanttu, «Finite Element Modeling of an Electrolysis Cell» Canadian Institute of Mining, Metallurgy and Pretroleum, pp. 561-573, 2007.

[8] E. P. Wiechmann, A. S. Morales, P. Aqueveque, and R. Mayne Nicholls, "Reducing Specific Energy to Shrink the Carbon Footprint in a Copper Electrowinning Facility", IEEE Trans. On. Ind. Appl., vol.47, n°3, pp.1175-1179, 2011.

[9] Wiechmann, E.P.; Morales, A.S.; Aqueveque, P.; Henríquez, J.A.; Muñoz, L.G., "3D FEM Thermal and Electrical Analysis of Copper Electrowinning Intercell Bars “, IEEE Transactions on Industry Applications, vol.53, no.1, pp.638-644, 2016.

[10] Wiechmann, E.P.; Morales, A.S.; Aqueveque, P.; Pino, E.; Muñoz, L.G. y Henríquez, J.A., "Intercell Busbar Design for Copper Electrowinning", IEEE Transactions on Industry Applications, vol.52, no.5, pp.4480-4488, 2016.

[11] E. P. Wiechmann, P. Aqueveque, J. A. Henriquez, L. G. Muñoz y A. Morales, «BMC: A Modulating Bar for Copper Electrowinning Designed for Heavy Duty and High Reliability, » IEEE Transactions on Industry Applications, vol. 50, nº 4, pp. 2375-2381, 2014.